



Cite this: *React. Chem. Eng.*, 2020, 5, 1104

Received 3rd April 2020,
Accepted 13th May 2020

DOI: 10.1039/d0re00133c

rsc.li/reaction-engineering

Revisiting the mechanism of the Fujiwara–Moritani reaction†

Christopher J. Mulligan,^a Jeremy S. Parker ^b and King Kuok (Mimi) Hii ^{*a}

The Fujiwara–Moritani reaction between *p*-methylacetanilide and *n*-butyl acrylate, catalysed by Pd(OAc)₂ in the presence of toluenesulfonic acid and benzoquinone, was (re-)investigated using reaction calorimetry and complementary spectroscopic methods. The (most) active catalyst was identified and the catalytic turnover rate was found to be independent of all stoichiometric reagents. Catalyst regeneration and deactivation pathways are discussed.

Introduction

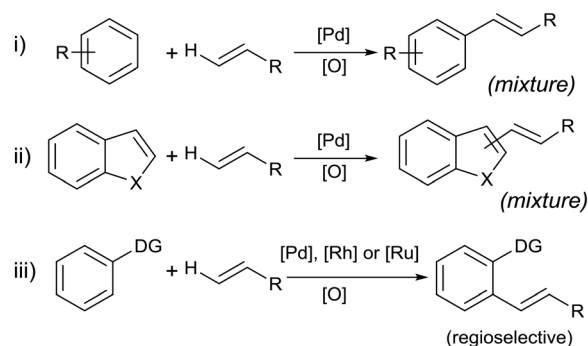
The Fujiwara–Moritani (F–M) reaction constitutes one of the earliest examples of a C–H activation reaction catalyzed by transition metals. The original report in 1967 described the reaction between a styrene–palladium chloride complex and benzene derivatives to form stilbenes.¹ Catalytic reactions were later accomplished by using Pd(OAc)₂ as a precursor for the olefination of simple (hetero)aromatic substrates (Scheme 1, eqn i and ii).^{2,3} In the early reports, oxygen gas was used in combination with copper or silver acetate to facilitate the dehydrogenative process, forming water as a by-product. In principle, the F–M reaction is more desirable than the Heck arylation reaction in terms of atom- and step-economies. In practice, however, the lack of a reactive centre poses problems such as poor regioselectivity and/or multiple substitutions of the olefin. Consequently, the F–M reaction was largely eschewed by the synthetic chemistry community, in favour of the Heck arylation reaction towards the end of the 20th century.

In the last decade, a resurgence in research activity for C–H activation reactions has led to renewed interest in the F–M reaction.^{2,4–6} One of the most significant breakthroughs is to deploy Lewis basic entities (‘directing groups’) on the arene substrate to control the substitution at the *ortho*-position (Scheme 1, eqn iii).^{7–10} In recent years, directing scaffolds were also used very effectively in controlling selective olefination at distal positions.^{11,12} Moreover, the reaction is no longer exclusive to Pd:Ru,^{13–18}

Rh^{19–23} and Ir²⁴ complexes have also been reported to be effective catalysts for certain systems.

In 1979, Horino and Inoue reported that anilides could undergo regioselective *ortho*-palladation with Pd(OAc)₂ to form palladacycles that can react with alkenes to form ‘Heck’ products.²⁵ More than two decades later, the catalytic reaction was demonstrated successfully by an industrial research team,²⁶ where the addition of benzoquinone (BQ) and toluenesulfonic acid (TsOH) effected the coupling between acetanilides (1) and acrylates (2) under mild reaction conditions (Scheme 2).

The F–M reaction is generally believed to proceed *via* a redox cycle (Scheme 3): initiating with a reaction between the Pd(II) salt and the acetanilide to produce a palladacycle **II**.²⁵ In the presence of an alkene, the complex undergoes migratory insertion and β-H elimination to afford the C–C coupled product and a hydridopalladium(II) intermediate (**III**). At this juncture, it is postulated complex **III** undergoes reductive elimination to produce acetic acid and a Pd(0) species, which is re-oxidised by BQ under acidic conditions,²⁷ to regenerate the active Pd(II) catalyst.



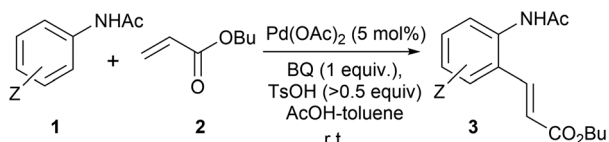
Scheme 1 General examples of the Fujiwara–Moritani (F–M) reaction.

^a Department of Chemistry, Molecular Sciences Research Hub, Imperial College London, 80, Wood Lane, London W12 0JQ, UK. E-mail: mimi.hii@imperial.ac.uk

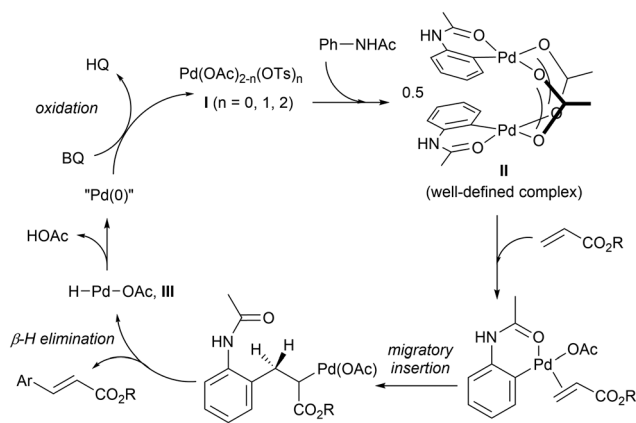
^b Early Chemical Development, Pharmaceutical Sciences, R&D, AstraZeneca, Macclesfield, UK

† Electronic supplementary information (ESI) available: Experimental procedures and additional data. See DOI: 10.1039/d0re00133c

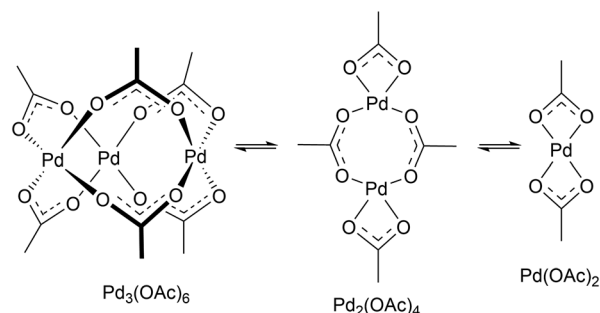




Scheme 2 The first reported example of the F–M reaction of acetanilides with butyl acrylate, catalysed by Pd(OAc)₂.



Scheme 3 Redox catalytic cycle proposed for the F–M reaction.



Scheme 4 Equilibrating forms of Pd(OAc)₂ in solution.

observed in the Fig. 1A suggests there is only one catalytically active species that is kinetically significant.

Effect of additive (*p*-toluenesulfonic acid)

Brønsted acid additives are commonly employed in many transition metal-catalysed C–H functionalisation reactions (for *e.g.* Cu,³³ Ru,³⁴ Co,³⁵ Rh,³⁶ Ir,³⁷ as well as Pd (ref. 38 and 39)) for a variety of reasons, although their roles in the

Results and discussion

In this work, we initiated a series of studies on the F–M reaction between 4-methylacetanilide (**1**, where Z = *para* Me) and butyl acrylate **2**, under similar conditions²⁸ to those reported by Boele *et al.*²⁶ (Scheme 2), with the aim to delineate the roles of, and synergistic effects between, the TsOH and BQ in the catalytic cycle, as well as the deactivation process(es).

Reaction order in Pd(OAc)₂

In this study, reaction progress was monitored using reaction calorimetry for reactions catalysed by ≥ 2.5 mol% of Pd(OAc)₂. At lower catalyst loadings (or where reactions were slow), aliquots were extracted and analysed by HPLC.

Pd(OAc)₂ is known to exist in monomeric, dimeric, trimeric forms in solution, depending on the solvent, and amount of additives and water present.²⁹ In acetic acid, the reaction solvent employed in F–M reaction, it is expected to be largely trimeric,³⁰ which can dissociate into dimeric and monomeric species in a rapid equilibrating process (Scheme 4).³¹

To determine whether all three forms of Pd(OAc)₂ could be catalytically active in the F–M reaction,³² the dependence of reaction rate on the [Pd] concentration was studied. By varying the catalyst loading between 2.5–10 mol% in the presence of 1 equivalent of TsOH, a linear plot of initial rates vs. [Pd(OAc)₂] (Fig. 1A) and an overlay of the plots of $v_{\text{obs}}/[\text{Pd}(\text{OAc})_2]$ vs. [1] (Fig. 1B) were obtained, showing that the reaction is first order with respect to [Pd]. The zero-intercept

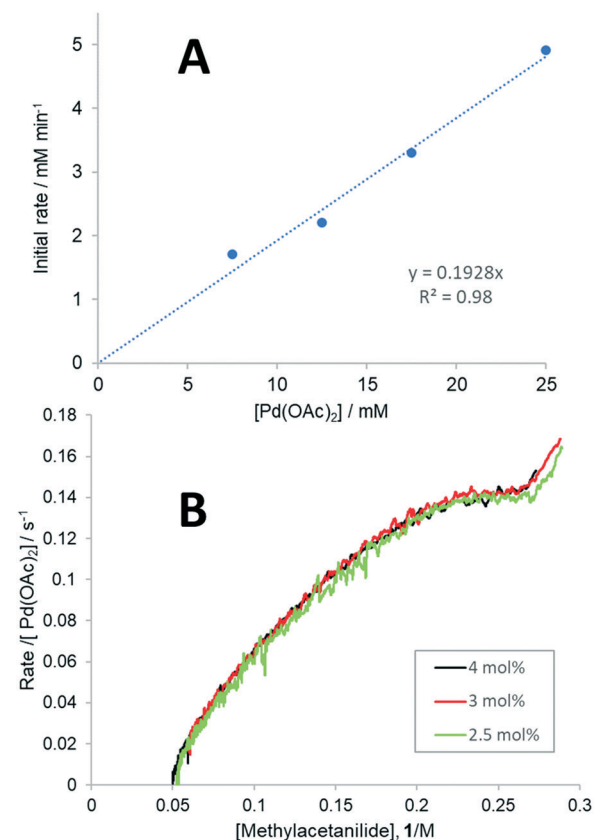


Fig. 1 Establishing [Pd] order. A: Plot of initial rates (extracted from HPLC analysis) vs. Pd(OAc)₂ concentrations between 2.5–10 mol%. B: Plots of rate/[Pd(OAc)₂] vs. [1] (obtained by reaction calorimetry) at three different Pd(OAc)₂ concentrations: 2.5–4 mol% (corresponding to 6.25–10 mM). Other reaction parameters: **1** (0.3 M), **2** (0.25 M), benzoquinone (0.25 M, 1 eq.)

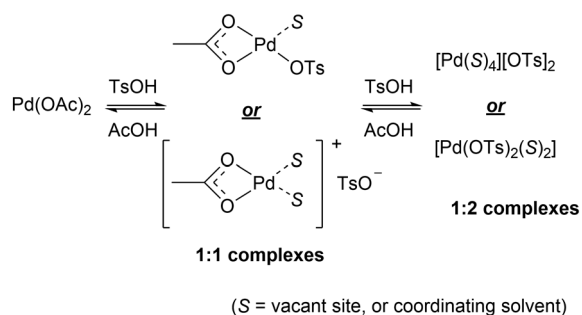


catalytic cycles are rarely studied. In the F–M reaction, the incorporation of 0.5–1 equivalent of *p*-toluenesulfonic acid (TsOH) has a dramatic effect on the catalytic turnover, allowing the reaction temperature to be lowered from 80 to 20 °C.²⁶ Indeed, during this work, the calorimetric studies were initiated by the addition of TsOH to mixtures of **1**, **2** and Pd(OAc)₂ which were thermally-equilibrated at 30 °C. It was suggested that the addition of the strong acid protonates an acetate ligand to generate catalytically active Pd(OAc)⁺; a hypothesis subsequently supported by a computational study by MacGregor and co-workers, who proposed an energetically-feasible acetate-assisted, concerted, metalation–deprotonation (CMD) mechanism for the C–H metalation step.⁴⁰ More recently, it has also been shown that the addition of carboxylic acids to Pd(OAc)₂ promotes the C–H activation step kinetically and thermodynamically.⁴¹

Interestingly, the F–M reaction can also proceed in the absence of carboxylate ions. In 2010, Nishikata and Lipshutz reported that oxidative *ortho*-olefination of electron-rich acetanilides can be effected at room temperature using cationic [Pd(MeCN)₄][BF₄]₂ as a catalyst precursor.^{42,43} In the same year, Brown and co-workers also reported that an isolated cationic cyclometalated complex containing a η¹-bound toluenesulfonate anion is catalytically active in the F–M reaction between acetanilides and methyl acrylate.⁴⁴ This led the authors to propose that [PdOTs]⁺ is able to activate the C–H bond of an acetanilide in the absence of acetate, *via* a ‘general base catalysis’ (GBC).⁴⁵

TsOH (pK_a –7) is a much stronger acid than AcOH (pK_a 4.7). Hence, we envisaged that TsOH can protonate Pd-bound acetate ligands to generate a mixture of 1:1⁴⁶ and 1:2⁴⁷ complexes in a facile equilibrium (Scheme 5). To delineate the role of the anionic ligands in the F–M reaction, kinetic experiments were performed with different amounts of [TsOH]. Between 15–37.4 mol% (Fig. 2 and S4, ESI[†]), the reaction displayed first order dependency on [TsOH]. Once again, the observation of a near-zero intercept in Fig. 2 suggests that while there may be more than one catalytically active species (Scheme 5), there is only one that may be kinetically relevant.

Above 50 mol% (reaction conditions), however, the reaction rate became independent of [TsOH] (saturation



Scheme 5 Ligand exchange between acetate and toluenesulfonate ions.

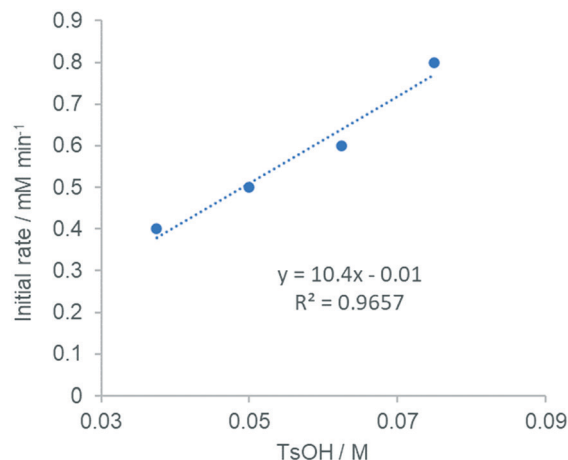


Fig. 2 Plot of initial rates vs. [TsOH] (between 15–30 mol%, extracted from HPLC analysis). For an RPKA analysis (between 2.5–37.5 mol%), see Fig. S2 (ESI[†]).

kinetics), implying a rapid equilibrium is reached between these homoleptic and heteroleptic species, compared to the turnover-limiting step.²⁶

Substituting TsOH with different *para*-substituted aryl sulfonic acids *p*-Z-C₆H₄SO₃H (where Z = CF₃, Me, OMe, 1 equivalent) has no discernible effects on the reaction rate (Fig. S1, ESI[†]). The addition of *p*-trifluoromethyl benzenesulfonic acid (Z = CF₃) to Pd(OAc)₂ in acetone-d₆ induced a δ¹⁹F shift (Fig. S6, ESI[†]), which can be used to construct a Job plot (continuous variation method): the resultant plot of Δδ vs. the mole fraction of the reactants displayed a maximum at 0.5 (Fig. 3), suggesting that the formation of a 1:1 complex is the most thermodynamically favourable; the curvature of the plot suggests a K_{eq} value > 100.⁴⁸

As may be expected, an attempt to reproduce the titration experiment in acetic acid did not produce any noticeable change in δ¹⁹F, as the equilibrium will favour the diacetate complex. Hence, in order for either Pd(OAc)⁺ or Pd(OTs)⁺ to

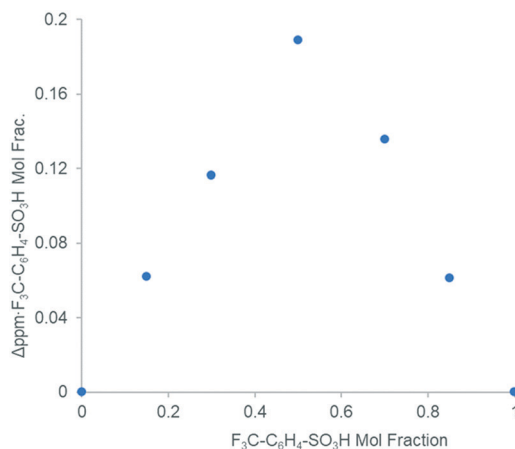


Fig. 3 Response in δ¹⁹F induced by the addition of *p*-trifluoromethanesulfonic acid to Pd(OAc)₂ in acetone (Job plot).



operate as active catalysts under the reaction conditions (where acetic acid is employed as a reaction solvent), they will need to be substantially more reactive than Pd(OAc)₂ (Curtin-Hammett principle). This is further supported by comparing kinetic rates, where the reaction catalysed by Pd(OTs)⁺ under acetate-free conditions (reported to be 0.115 mM min⁻¹ in acetone-d₆)⁴⁴ is approximately 20 times slower than the reaction performed with Pd(OAc)₂/TsOH in acetic acid (2 mM min⁻¹, present work). Combined with the result of the Job plot, and the absence of any *para*-substituent effect on the aryl sulfonate anion, we conclude that Pd(OAc)⁺ is likely to be a more active catalyst than Pd(OTs)⁺ under the reaction conditions.

Catalyst deactivation

A series of 'same excess' experiments⁴⁹ were performed to probe the catalyst stability towards different reaction components (Table 1).

Experiments 1 and 2 were performed with different initial concentrations of acrylate 2 (0.25 and 0.175 M, respectively), maintaining the same excess of the acetanilide 1 (0.05 M). The resultant plots (Fig. 4A) showed that experiment 2 proceeds with a faster reaction rate than experiment 1, indicative of the catalyst deactivation. This can be attributed entirely to the presence of products (experiment 5, Fig. 4B). Subsequent addition of each of the two reaction products, hydroquinone (HQ) and 3 (experiments 3 and 4, respectively), showed that the HQ has a stronger inhibitory effect than the substituted alkene 3 (Fig. S5, ESI[†]).

The good overlap between the curves in Fig. 4B also shows that other catalyst deactivation pathways, such as the formation of Pd black, is not significant under these reaction conditions.

Completing the cycle: regeneration of the active catalyst

BQ is believed to have dual roles in this process,⁵¹ acting as an oxidant and a ligand to stabilize the low valent-Pd, preventing it from degradation to Pd black. It was also proposed that following β-hydride elimination, the resultant AcO-Pd-H intermediate **III** (Scheme 3) is reduced to a BQ-stabilised Pd(0) species, which is regenerated to Pd(II) by BQ in the presence of acetic acid – a computational study of this process by López and Maseras showed that the transformation of (η⁶-BQ)Pd(AcOH)₂ to Pd(OAc)₂ can occur *via*

Table 1 Reaction conditions for 'same excess' experiments^a

Components	[1]/M	[2]/M	[3]/M	[HQ]/M
Expt 1: initial conditions	0.3	0.25	0	0
Expt 2: 'same excess'	0.175	0.125	0	0
Expt 3: 'same excess' + HQ	0.175	0.125	0	0.125
Expt 4: 'same excess' + [3]	0.175	0.125	0.125	0
Expt 5: 'same excess' + HQ + [3]	0.175	0.125	0.125	0.125

^a Pd(OAc)₂ (12.5 mM, 5 mol%), TsOH (0.125 M, 0.5 eq.), BQ (0.25 M, 1 eq.), 30 °C, AcOH.

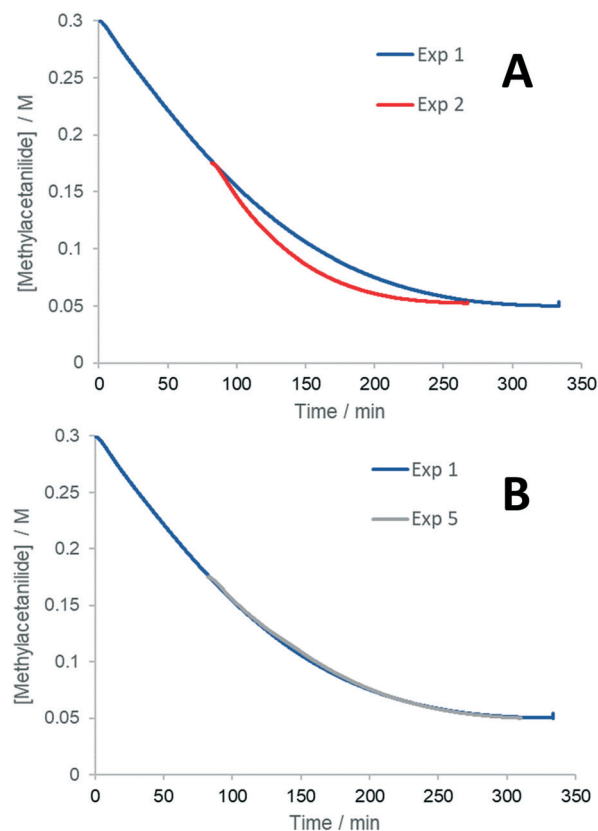
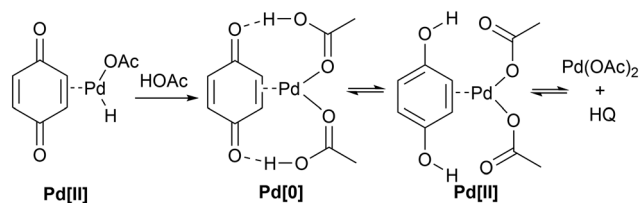


Fig. 4 Results of 'same excess' experiments (Table 1).

consecutive hydrogen transfer from AcOH to BQ (Scheme 6) – the energies were computed to be 92.1 kJ mol⁻¹, and 65.7 kJ mol⁻¹ for the reverse (dehydrogenative) process.⁵⁰ The low energy associated with the dehydrogenative step will account for the observed HQ inhibition of the catalyst.

Rate dependence on the concentration of reactants

In the previous study by the de Vries group,²⁶ the electrophilic attack of the cationic Pd(OAc)⁺ on the arene ring was proposed to be the turnover-limiting step, based on the following observations: i) the F-M reaction proceeds faster with electron-rich acetanilides (Hammett correlation); ii) observation of a significant kinetic isotope effect ($k_D/k_H = 3$; established by comparing k_{obs} obtained from using acetanilide-*h*₅ and *d*₅); and iii) the reaction between the



Scheme 6 Regeneration of Pd(OAc)₂ *via* a redox pathway involving H-transfer, proposed by López and Maseras.⁵⁰



isolated palladacycle complex **II** with the olefin is an order of magnitude faster than the equivalent reaction using the catalyst generated *in situ*. In the study by Brown *et al.*, conducted in the absence of acetate-ions,⁴⁴ the reaction also exhibited first order dependency on acetanilide, zero order in BQ and a modest effect of the alkenes, which also supports a turnover-limiting metalation step.

Thus, we were rather surprised to find that the rate of the reaction is, in fact, independent of the initial acetanilide concentration (Fig. 5). Subsequently, the reaction rate was also shown to be independent of the initial concentrations of the alkene and BQ (Fig. S2 and S3, ESI†).

The apparent zero-order in acetanilide may be explained by the existence of an acetanilide-bound complex (**IV**) immediately prior to the rate-limiting cyclometalation step (Scheme 7). The proposal will also explain why the heteroleptic $[\text{Pd}(\text{OAc})][\text{OTs}]$ complex is more active than the corresponding ditosylate or diacetate salts, as it contains a labile OTs that can be displaced easily by the acetanilide substrate to form complex **IV**.

Kinetic modelling

The initiating steps of the updated catalytic cycle shown in Scheme 7 is reminiscent of the Michaelis–Menten mechanism, where the reaction is dominated by a reversible binding of the substrate (acetanilide) to the active metal centre (K_1) to form complex **IV**, prior to slow, irreversible C–H bond cleavage to form the cyclometalated complex **II** (k_2), which undergoes spontaneous C–C coupling (zero order in alkene) to generate the product **3** and the hydridopalladium intermediate (k_3). BQ then participates in the regeneration of the active catalyst, which can be inhibited by the HQ by-product (K_4).

A microkinetic model of these elementary steps can be constructed from the reaction intermediates and reactants, incorporating six discrete rate constants (Scheme 8). Using an ordinary differential equation (ODE) solver, the data

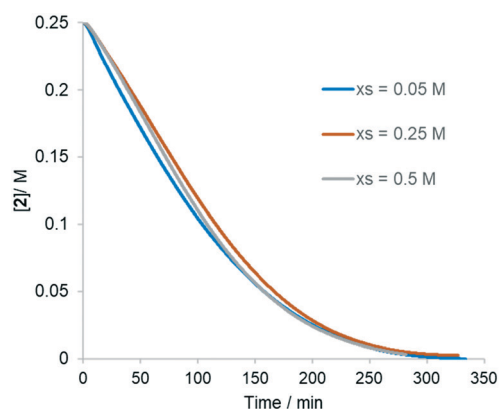
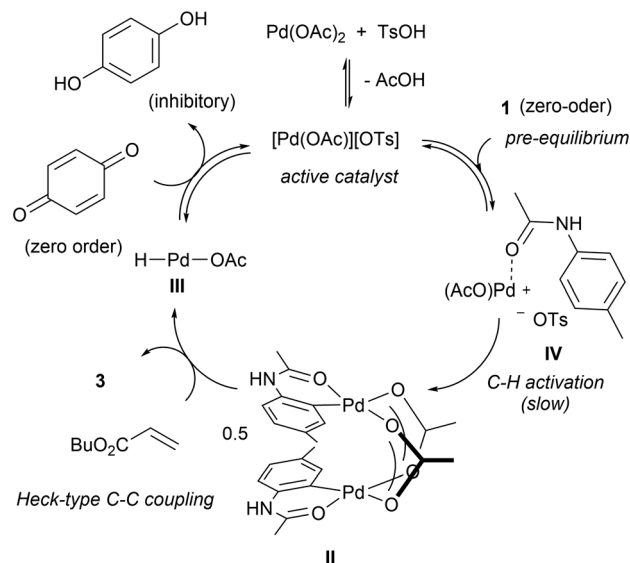


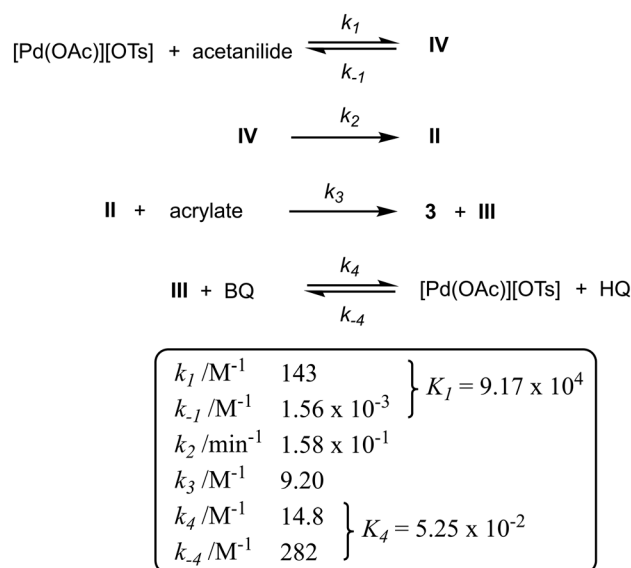
Fig. 5 Rate curve showing that the reaction rate is independent of [1]. Reaction conditions: butyl acrylate **2** (0.25 M), BQ (0.25 M), TsOH (0.125 M), $\text{Pd}(\text{OAc})_2$ (12.5 mM, 5 mol%). Legend: 0.30 M (0.05 M excess), 0.50 M (0.25 M excess) and 0.75 M (0.5 M excess) of [1].



Scheme 7 Revised catalytic cycle for the F–M reaction.

gathered from 16 independent kinetic experiments were fitted to the model, from which the rate constants can be extracted (Fig. S7–S9, ESI†).

A good fit between the simulated and experimental data suggests that catalyst decomposition (*e.g.* formation of inactive Pd black) is not a significant process under these reaction conditions, as was previously verified by the ‘same excess’ experiments (Fig. 4 and S5†). While the rate constants confirmed k_2 as the turnover-limiting step (as expected), it is interesting to note the magnitudes of the two equilibrium processes: K_4 (0.05) \ll K_1 (9.17×10^4), suggesting that the stronger binding of the acetanilide (compared to HQ) to the $[\text{Pd}(\text{OAc})][\text{OTs}]$ provides the driving force for the turnover.



Scheme 8 Kinetic modelling and kinetic constants (with reference to Scheme 7).



Towards the end of the reaction, as the concentration of acetanilide is depleted, the binding of the HQ by-product become competitive, leading to catalyst inhibition.

Role of the terminal oxidant (BQ vs. O₂)

Benzoquinone is widely implicated in the catalyst regeneration step. It has an important role in stabilising the monometallic Pd species, thus preventing the aggregation of Pd that leads to the formation of catalytically inactive Pd black. In the studies described above, a stoichiometric amount of BQ was employed. Under these conditions, the formation of Pd black was not a competitive process.

However, the use of BQ as a stoichiometric reagent is unattractive in terms of the atom-economy. BQ and HQ are known irritants and possible carcinogens, so it will be desirable to reduce or replace them with safer oxidants. Previously, Pd-catalyzed F–M reactions have been reported to proceed under high O₂ pressures (>8 bar) and elevated temperatures with an excess of the arene reactant.^{52–54} Encouraged by these accounts, we attempted to replace BQ with O₂. However, our efforts were thwarted by highly capricious results: in the absence of BQ, a large variation of reaction yields between 11 to >95% were obtained from twenty-two individual, but identical reaction mixtures conducted under aerobic conditions. Speculating that diffusion of gaseous O₂ into the liquid-phase may be the cause of the irreproducibility, reactions were repeated up to five times, in parallel, on a larger scale with mechanical (overhead) stirrers (STEM Integrity10 Reaction Station), varying the stirring rate between 350–1200 rpm. In all cases, no correlation between reaction yield and stirring speed/reaction vessel can be established. In this part of the study, the formation of Pd black was observed in the early stages of the reaction, irrespective of the reaction outcome. This led us to postulate that, in the absence of BQ, Pd aggregation occurs readily to form a ‘cocktail’ of interchanging Pd species, including complexes, colloids/clusters and nanoparticles⁵⁵ – a highly stochastic system that is difficult to control and replicate using stirred glass reactors and ambient temperature and pressure.⁵⁶ Indeed, reproducibility of the reaction could only be achieved by the addition of at least 50 mol% of BQ or 20 mol% of Cu(OAc)₂ (as a redox mediator).

Conclusions

The work provides new insights to the kinetic profile of the F–M reaction (Schemes 7 vs. 3). In the presence of TsOH, a heteroleptic [Pd(OAc)](OTs) complex is generated, which is catalytically more active than either Pd(OAc)₂ or Pd(OTs)₂. The F–M reaction was found to operate under saturation (Michaelis–Menten) kinetics, where zero order rate dependencies were observed for all the stoichiometric reagents (acetanilide, acrylate and BQ). This is attributed to the reversible binding of the acetanilide substrate to the catalytically active Pd species, prior to a slow intramolecular C–H activation step. Subsequent kinetic modelling revealed that competitive binding between

the acetanilide and HQ to the active catalyst is also important in achieving catalytic turnover.

Irreversible catalyst deactivation occurs through the Pd aggregation, which can be prevented by the addition of BQ or Cu salts. In the present work, the coupling between 1 and 2 were attempted under aerobic conditions (in the absence of BQ or redox mediators). Under ambient conditions, quantitative conversions can be obtained in some instances, but the reaction outcome was found to be hugely irreproducible, possibly due to the highly stochastic nature of the Pd–Pd aggregation process and the difficulty in controlling the delivery of O₂ to the solution under ambient conditions. Understanding the causes and control of these processes will be important in the future development of atom-economical and sustainable oxidative coupling reactions under ambient, aerobic conditions.

Conflicts of interest

There are no conflicts to declare.

Acknowledgements

We thank the EPSRC and AstraZeneca for studentship support. Part of this work (calorimetry and parallel reaction screening) was conducted during CJM's industrial placement at AstraZeneca's R&D site at Macclesfield, UK. We are grateful to Dr Jordi Bures (University of Manchester) for helpful comments on this manuscript.

Notes and references

- 1 I. Moritani and Y. Fujiwara, Aromatic substitution of styrene-palladium chloride complex, *Tetrahedron Lett.*, 1967, **8**, 1119–1122.
- 2 T. Kitamura and Y. Fujiwara, Dehydrogenative Heck-type reactions: the Fujiwara-Moritani reaction, *RSC Green Chem. Ser.*, 2015, **26**, 33–54.
- 3 Y. Fujiwara, I. Moritani, S. Danno, R. Asano and S. Teranishi, Aromatic substitution of olefins. VI. Arylation of olefins with palladium(II) acetate, *J. Am. Chem. Soc.*, 1969, **91**, 7166–7169.
- 4 C. Liu, J. W. Yuan, M. Gao, S. Tang, W. Li, R. Y. Shi and A. W. Lei, Oxidative coupling between two hydrocarbons: an update of recent C–H functionalizations, *Chem. Rev.*, 2015, **115**, 12138–12204.
- 5 E. M. Ferreira, H. Zhang and B. M. Stoltz, in *The Mizoroki-Heck Reaction*, ed. M. Oestreich, John Wiley & Sons, 2009, ch. 9, pp. 345–382.
- 6 L. H. Zhou and W. J. Lu, Towards ideal synthesis: alkenylation of aryl C–H bonds by a Fujiwara-Moritani reaction, *Chem. – Eur. J.*, 2014, **20**, 634–642.
- 7 S. I. Gorelsky, Origins of regioselectivity of the palladium-catalyzed (aromatic)C–H bond metalation-deprotonation, *Coord. Chem. Rev.*, 2013, **257**, 153–164.
- 8 H. Choi, M. Min, Q. Peng, D. Kang, R. S. Paton and S. Hong, Unraveling innate substrate control in site-selective



- palladium-catalyzed C-H heterocycle functionalization, *Chem. Sci.*, 2016, 7, 3900–3909.
- 9 W. Ma, P. Gandeepan, J. Li and L. Ackermann, Recent advances in positional-selective alkenylations: removable guidance for twofold C–H activation, *Org. Chem. Front.*, 2017, 4, 1435–1467.
 - 10 H. Chen, P. Wedi, T. Meyer, G. Tavakoli and M. van Gemmeren, Dual ligand-enabled nondirected C–H olefination of arenes, *Angew. Chem., Int. Ed.*, 2018, 57, 2497–2501.
 - 11 S. Bag and D. Maiti, Palladium-catalyzed olefination of aryl C–H bonds by using directing scaffolds, *Synthesis*, 2016, 48, 804–815.
 - 12 R. Sharma and U. Sharma, Remote C–H bond activation/transformations: A continuous growing synthetic tool; Part II, *Catal. Rev.: Sci. Eng.*, 2018, 60, 497–565.
 - 13 R. Manikandan, P. Madasamy and M. Jeganmohan, Ruthenium-catalyzed ortho alkenylation of aromatics with alkenes at room temperature with hydrogen evolution, *ACS Catal.*, 2016, 6, 230–234.
 - 14 R. Das and M. Kapur, Fujiwara-Moritani reaction of Weinreb amides using a ruthenium-catalyzed C–H functionalization reaction, *Chem. – Asian J.*, 2015, 10, 1505–1512.
 - 15 R. Das and M. Kapur, Product control using substrate design: ruthenium-catalysed oxidative C–H olefinations of cyclic weinreb amides, *Chem. – Eur. J.*, 2016, 22, 16984–16988.
 - 16 K. Graczyk, W. Ma and L. Ackermann, Oxidative alkenylation of aromatic esters by ruthenium-catalyzed twofold C–H bond cleavages, *Org. Lett.*, 2012, 14, 4110–4113.
 - 17 Y. Y. Ping, Z. B. Chen, Q. P. Ding, Q. Zheng, Y. Q. Lin and Y. Y. Peng, Ru-catalyzed ortho-oxidative alkenylation of 2-arylbenzo d thiazoles in aqueous solution of anionic surfactant sodium dodecylbenzenesulfonate (SDBS), *Tetrahedron*, 2017, 73, 594–603.
 - 18 Y. C. Yuan, C. Bruneau, T. Roisnel and R. Gramage-Doria, Site-selective Ru-catalyzed C–H bond alkenylation with biologically relevant isoindolinones: a case of catalyst performance controlled by subtle stereo-electronic effects of the weak directing group, *Catal. Sci. Technol.*, 2019, 9, 4711–4717.
 - 19 X. Xue, J. Xu, L. Zhang, C. Xu, Y. Pan, L. Xu, H. Li and W. Zhang, Rhodium(III)-catalyzed direct c-h olefination of arenes with aliphatic olefins, *Adv. Synth. Catal.*, 2016, 358, 573–583.
 - 20 X.-G. Liu, H. Gao, S.-S. Zhang, Q. Li and H. Wang, N–O bond as external oxidant in group 9 Cp*M(III)-catalyzed oxidative C–H coupling reactions, *ACS Catal.*, 2017, 7, 5078–5086.
 - 21 C. Xia, A. J. P. White and K. K. Hii, Synthesis of isoindolinones by Pd-catalyzed coupling between N-methoxybenzamide and styrene derivatives, *J. Org. Chem.*, 2016, 81(17), 7931–7938.
 - 22 W. D. Lin, W. Q. Li, D. D. Lu, F. Su, T. B. Wen and H. J. Zhang, Dual effects of cyclopentadienyl ligands on Rh(III)-catalyzed dehydrogenative arylation of electron-rich alkenes, *ACS Catal.*, 2018, 8, 8070–8076.
 - 23 Q. S. Han, X. M. Guo, Z. Y. Tang, L. Su, Z. Z. Yao, X. F. Zhang, S. Lin, S. C. Xiang and Q. F. Huang, Rhodium-catalyzed regioselective ortho C–H olefination of 2-arylindoles via nh-indole-directed C–H bond cleavage, *Adv. Synth. Catal.*, 2018, 360, 972–984.
 - 24 P. Cooper, G. E. M. Crisenza, L. J. Feron and J. F. Bower, Iridium-catalyzed alpha-selective arylation of styrenes by dual C–H functionalization, *Angew. Chem., Int. Ed.*, 2018, 57, 14198–14202.
 - 25 H. Horino and N. Inoue, Ortho-vinylation of anilines via cyclopalladation - new route to nitrogen-heterocycles, *Tetrahedron Lett.*, 1979, 2403–2406.
 - 26 M. D. K. Boele, G. P. F. van Strijdonck, A. H. M. de Vries, P. C. J. Kamer, J. G. de Vries and P. W. N. M. van Leeuwen, Selective Pd-catalyzed oxidative coupling of anilides with olefins through C–H bond activation at room temperature, *J. Am. Chem. Soc.*, 2002, 124, 1586–1587.
 - 27 B. P. Babu, X. Meng and J.-E. Bäckvall, Aerobic oxidative coupling of arenes and olefins through a biomimetic approach, *Chem. – Eur. J.*, 2013, 19, 4140–4145.
 - 28 The reaction was conducted isothermally at 30 °C to counteract fluctuations in ambient temperature. A slight excess of the acetanilide was also employed to suppress the formation of the di-olefinated product.
 - 29 W. A. Carole and T. J. Colacot, Understanding palladium acetate from a user perspective, *Chem. – Eur. J.*, 2016, 22, 7686–7695.
 - 30 R. N. Pandey and P. M. Henry, Interaction of palladium(II) acetate with sodium and lithium acetate in acetic-acid, *Can. J. Chem.*, 1974, 52, 1241–1247.
 - 31 L. A. Adrio, B. N. Nguyen, G. Guilera, A. G. Livingston and K. K. Hii, Deconvolution of the mechanism of homogeneous gold-catalyzed reactions, *Catal. Sci. Technol.*, 2012, 2, 316–323.
 - 32 J. Vana, J. Hanusek and M. Sedlak, Bi and trinuclear complexes in palladium carboxylate-assisted C–H activation reactions, *Dalton Trans.*, 2018, 47, 1378–1382.
 - 33 K.-S. Masters, T. R. M. Rauws, A. K. Yadav, W. A. Herrebout, B. Van der Veken and B. U. W. Maes, On the importance of an acid additive in the synthesis of pyrido[1,2-a]benzimidazoles by direct copper-catalyzed amination, *Chem. – Eur. J.*, 2011, 17, 6315–6320.
 - 34 J. B. C. Mack, J. D. Gipson, J. Du Bois and M. S. Sigman, Ruthenium-catalyzed C–H hydroxylation in aqueous acid enables selective functionalization of amine derivatives, *J. Am. Chem. Soc.*, 2017, 139, 9503–9506.
 - 35 X. X. Shi, W. Y. Xu, R. C. Wang, X. F. Zeng, H. Y. Qiu and M. Wang, Ketone-directed cobalt(III)-catalyzed regioselective C2 amidation of indoles, *J. Org. Chem.*, 2020, 85, 3911–3920.
 - 36 Y. Sun and N. Cramer, Enantioselective synthesis of chiral-at-sulfur 1,2-benzothiazines by Cp*Rh(III)-catalyzed C–H functionalization of sulfoximines, *Angew. Chem., Int. Ed.*, 2018, 57, 15539–15543.
 - 37 D. Xing, X. T. Qi, D. Marchant, P. Liu and G. B. Dong, Branched-selective direct-alkylation of cyclic ketones with simple alkenes, *Angew. Chem., Int. Ed.*, 2019, 58, 4366–4370.



- 38 X.-H. Liu, H. Park, J.-H. Hu, Y. Hu, Q.-L. Zhang, B.-L. Wang, B. Sun, K.-S. Yeung, F.-L. Zhang and J.-Q. Yu, Diverse ortho-C(sp²)-H Functionalization of Benzaldehydes Using Transient Directing Groups, *J. Am. Chem. Soc.*, 2017, **139**, 888–896.
- 39 Y. Xiong, T. Besset, D. Cahard and X. Pannecoucke, Palladium(II)-catalyzed directed trifluoromethylthiolation of unactivated C(sp³)-H bonds, *J. Org. Chem.*, 2015, **80**, 4204–4212.
- 40 D. L. Davies, S. M. A. Donald and S. A. Macgregor, Computational study of the mechanism of cyclometalation by palladium acetate, *J. Am. Chem. Soc.*, 2005, **127**, 13754–13755.
- 41 J. Vana, J. Bartacek, J. Hanusek, J. Roithova and M. Sedlak, Bi and trinuclear complexes in palladium carboxylate-assisted C-H activation reactions, *J. Org. Chem.*, 2019, **84**, 12746–12754.
- 42 Note that in this case, both BQ (1 equiv.) and AgNO₃ (2 equiv.) were employed as oxidants.
- 43 T. Nishikata and B. H. Lipshutz, Cationic Pd(II)-catalyzed Fujiwara-Moritani reactions at room temperature in water, *Org. Lett.*, 2010, **12**, 1972–1975.
- 44 W. Rauf, A. L. Thompson and J. M. Brown, Anilide activation of adjacent C-H bonds in the palladium-catalyzed Fujiwara-Moritani reaction, *Dalton Trans.*, 2010, **39**, 10414–10421.
- 45 W. Rauf and J. M. Brown, Palladium-catalyzed directed C-H activation by anilides and ureas; water participation in a general base mechanism, *Org. Biomol. Chem.*, 2016, **14**, 5251–5257.
- 46 Attempts to isolate this mixed-ligand Pd species resulted in its decomposition to Pd black.
- 47 C. E. Houlden, C. D. Bailey, J. G. Ford, M. R. Gagné, G. C. Lloyd-Jones and K. I. Booker-Milburn, Distinct reactivity of Pd(OTs)₂: the intermolecular Pd(II)-catalyzed 1,2-carboamination of dienes, *J. Am. Chem. Soc.*, 2008, **130**, 10066–10067.
- 48 J. S. Renny, L. L. Tomasevich, E. H. Tallmadge and D. B. Collum, Method of continuous variations: applications of Job plots to the study of molecular associations in organometallic chemistry, *Angew. Chem., Int. Ed.*, 2013, **52**, 11998–12013.
- 49 D. G. Blackmond, Kinetic profiling of catalytic organic reactions as a mechanistic tool, *J. Am. Chem. Soc.*, 2015, **137**, 10852–10866.
- 50 J. J. Plata, M. García-Mota, A. A. C. Braga, N. López and F. Maseras, Vinyl acetate synthesis on homogeneous and heterogeneous Pd-based catalysts: a theoretical analysis on the reaction mechanisms, *J. Phys. Chem. A*, 2009, **113**, 11758–11762.
- 51 A. Vasseur, J. Muzart and J. Le Bras, Ubiquitous benzoquinones, multitasking compounds for palladium-catalyzed oxidative reactions, *Eur. J. Org. Chem.*, 2015, **2015**, 4053–4069.
- 52 R. S. Shue, Catalytic coupling of aromatics and olefins by homogeneous palladium(II) compounds under oxygen, *J. Chem. Soc. D*, 1971, 1510–1511.
- 53 J. Hajek, M. Dams, C. Detrembleur, R. Jerome, P. A. Jacobs and D. E. De Vos, Heterogeneous alkenylation of aromatics under oxygen, *Catal. Commun.*, 2007, **8**, 1047–1051.
- 54 M. Dams, D. E. De Vos, S. Celen and P. A. Jacobs, Toward waste-free production of Heck products with a catalytic palladium system under oxygen, *Angew. Chem., Int. Ed.*, 2003, **42**, 3512–3515.
- 55 D. B. Eremin and V. P. Ananikov, Understanding active species in catalytic transformations: From molecular catalysis to nanoparticles, leaching, "Cocktails" of catalysts and dynamic systems, *Coord. Chem. Rev.*, 2017, **346**, 2–19.
- 56 High temperatures and pressures for aerobic processes were avoided for safety reasons, see: A. Gavriilidis, A. Constantinou, K. Hellgardt, K. K. Hii, G. Hutchings, G. Brett, S. Kuhn and S. P. Marsden, *React. Chem. Eng.*, 2016, **1**, 595–612.

